

Production of charmed mesons in $\gamma\gamma$ interactions ^{*}

TASSO Collaboration

W. Braunschweig, R. Gerhards, F.J. Kirschfink,
H.-U. Martyn

I. Physikalisches Institut der RWTH, Aachen,
Federal Republic of Germany^a

B. Bock¹, H.M. Fischer, H. Hartmann, J. Hartmann,
E. Hilger, A. Jocksch², R. Wedemeyer

Physikalisches Institut der Universität, Bonn,
Federal Republic of Germany^a

B. Foster, A.J. Martin³

H.H. Wills Physics Laboratory, University of Bristol,
Bristol, UK^b

E. Bernardi⁴, J. Chwastowski⁵, A. Eskreys⁵,
K. Genser⁶, H. Hultschig, P. Joos, H. Kowalski,
A. Ladage, B. Löhner, D. Lüke, D. Notz, J.M. Pawlak⁶,
K.-U. Pösnecker, E. Ros, D. Trines, R. Walczak⁶,
G. Wolf

Deutsches Elektronen-Synchrotron DESY, Hamburg,
Federal Republic of Germany

H. Kolanoski

Institut für Physik, Universität, Dortmund,
Federal Republic of Germany^a

T. Kracht⁷, J. Krüger, E. Lohrmann, G. Poelz,
W. Zeuner⁸

II. Institut für Experimentalphysik der Universität, Hamburg,
Federal Republic of Germany^a

J. Hassard, J. Shulman⁹, D. Su¹⁰, I.R. Tomalin
Department of Physics, Imperial College, London, UK^b

F. Barreiro, A. Leites, J. del Peso
Universidad Autonoma de Madrid, Madrid, Spain^c

J.C. Hart, D.H. Saxon
Rutherford Appleton Laboratory, Chilton, Didcot, UK^b

S. Brandt, M. Holder
Fachbereich Physik der Universität-Gesamthochschule, Siegen,
Federal Republic of Germany^a

E. Duchovni, Y. Eisenberg¹¹, D. Hochman,
U. Karshon, L. Lyons¹², A. Montag, D. Revel,
E.E. Ronat¹³, N. Wainer
Weizmann Institute, Rehovot, Israel^d

D. Muller¹⁴, S. Ritz¹⁵, D. Strom¹⁶, M. Takashima⁸,
Sau Lan Wu, G. Zobernig
Department of Physics, University of Wisconsin, Madison, WI,
USA^e

Received 2 April 1990

^{*} This paper is dedicated to the memory of our friend and colleague
Elhanan (Ed) Ronat

¹ Now at Krupp Atlas Elektr. GmbH, Bremen, FRG

² Now at Fa. Fichtner, Stuttgart, FRG

³ Now at Queen Mary and Westfield College, London, UK

⁴ Now at Robert Bosch GmbH, Schieberdingen, FRG

⁵ Now at Inst. of Nuclear Physics, Cracow, Poland

⁶ Now at Warsaw University, Poland; partially supported by
grant CPBP 01.06

⁷ Now at Hasylab, DESY

⁸ Now at CERN, Geneva, Switzerland

⁹ Now at University College, London

¹⁰ Now at RAL, Chilton, Didcot, UK

¹¹ The Nicki and J. Ira Harris professorial chair

¹² Visitor from Nuclear Physics Lab., Oxford, UK

¹³ Deceased

¹⁴ Now at SLAC, Stanford, USA

¹⁵ Now at Columbia University, NY, USA

¹⁶ Now at University of Chicago, Chicago, IL, USA

^a Supported by Bundesministerium für Forschung und Technologie

^b Supported by UK Science and Engineering Research Council

^c Supported by CAICYT

^d Supported by the Minerva Gesellschaft für Forschung GmbH

^e Supported by US Dept. of Energy, contract DE-AC02-76ER000881 and by US Nat. Sci. Foundation Grant no INT-8313994 for travel

Abstract. Production of charmed mesons in $\gamma\gamma$ -interactions at PETRA energies has been observed in the TASSO detector. Cross sections for inclusive $D^{*\pm}$ and $D^0\bar{D}^0$ production have been measured. Neutral and charged meson pairs are estimated to be produced with comparable cross sections, and their sum seems to account for a sizeable fraction of $\sigma_{\text{tot}}(\gamma\gamma \rightarrow \text{hadrons})$ near the $c\bar{c}$ threshold.

1 Introduction

Photon-photon reactions involving charmed quarks in the final state, as given schematically in Fig. 1 a, provide tests of production mechanism models for $\gamma\gamma$ interactions. Studies of η_c production have already been published [1]. Here we report on the production of open charm mesons. The search includes two types of processes: inclusive $D^{*\pm}$ production and $D^0\bar{D}^0$ pair production. Inclusive $D^{*\pm}$ production in $\gamma\gamma$ reactions has already been reported by JADE [2] and by the TPC/Two-Gamma Collaboration [3].

Since the $\rho^0\rho^0$ [4] and the $K^{*+}K^{*-}$ [4, 5] cross sections near threshold are considerably larger than expected, it is of interest to see whether charm production has a similar threshold enhancement. A measurement of the ratio between charged and neutral charmed meson pairs may also help in determining the relative importance of the different production processes (Fig. 1).

In this paper we report the observation of the reactions

$$\gamma\gamma \rightarrow D^{*+} + X; \quad D^{*+} \rightarrow D^0 \pi^+ \quad (1)$$

and

$$\gamma\gamma \rightarrow D^0 \bar{D}^0 (+X). \quad (2)$$

For identifying the D^0 in both reactions we have used the decay modes

$$D^0 \rightarrow K^- \pi^+ \quad [3.8 \pm 0.4\%] \quad (3)$$

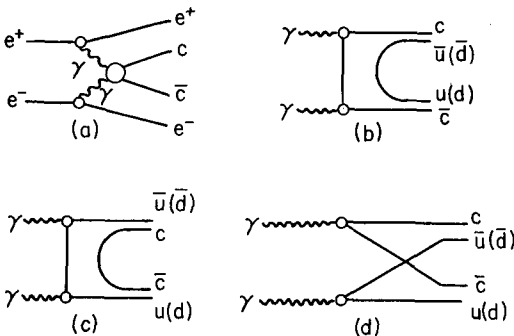


Fig 1 a-d. Diagrams contributing to $\gamma\gamma$ -charm production. **a** inclusive, **b**, **c** box diagrams yielding $D^\pm/D^0(D^{*\pm}/D^{*0})=1:1$ **b**, or $1:16$ **c**. Note that **c** is expected to be suppressed because of the small $c\bar{c}$ sea. **d** quark exchange diagram, yielding $1:4$ for above ratio. Such a diagram is expected to interfere with **b**

and

$$D^0 \rightarrow K^- \pi^+ \pi^+ \pi^- \quad [7.9 \pm 1.0\%] \quad (4)$$

where the numbers in brackets are the relevant branching ratios [6]. For reaction (2) we have also searched for the decay modes

$$D^0 \rightarrow K^- \pi^+ \pi^0 \quad [12.5 \pm 1.4\%] \quad (5)$$

and

$$D^0 \rightarrow \bar{K}^0 \pi^+ \pi^- \quad [5.6 \pm 0.7\%]; \quad K^0 \rightarrow \pi^+ \pi^-. \quad (6)$$

In all cases, corresponding processes where every particle is replaced by its antiparticle are included.

2 Data

Our data sample comes from two run periods: an integrated luminosity of 83 pb^{-1} was taken at PETRA during 1979–1982 at various beam energies where most of the data is around $E_b=17 \text{ GeV}$. An integrated luminosity of 106 pb^{-1} was taken in 1986 at a fixed beam energy of $E_b=17.5 \text{ GeV}$. The 1986 data has an improved accuracy of track parameters due to the TASSO high precision vertex detector (VXD). A general description of the TASSO detector and the vertex chamber can be found in [7, 8] respectively. In order to improve the momentum resolution, the average beam position was used as an additional constraint [9] in fitting charged tracks from the primary vertex. No requirement has been made on the detection of the scattered e^+ and/or e^- in the final state.

The most effective trigger for low multiplicity $\gamma\gamma$ events required two track candidates in the central drift chamber (DC) found by a hardware preprocessor, containing hit information from the DC, the time-of-flight (TOF) counters, the central proportional chamber (CPC), and, for the second run period, the VXD. In addition the information on the z coordinates of tracks from the CPC-cathode readout was used in this trigger. Other triggers, requiring at least 4 charged tracks or 2 back-to-back tracks were also used. The trigger efficiency per track varied as a function of the track momentum component, P_T , transverse to the beam direction. For the first run period this efficiency reached a value of $\sim 95\%$ for $P_T > 0.29 \text{ GeV}/c$, while for the second period it was $\sim 70\%$ for $P_T > 0.22 \text{ GeV}/c$.

In order to select $\gamma\gamma$ charmed events, we required:

- i) The sum of the measured charged particle momenta to be $2.4 \text{ GeV}/c < \sum |\mathbf{P}| < 10 \text{ GeV}/c$, ($< 8 \text{ GeV}/c$) for reaction (1) (reaction (2)); this is to suppress the e^+e^- annihilation reactions and reduce non-charm background. For reaction (1), a cut on the observed longitudinal momentum $|\Sigma P_z| < 5 \text{ GeV}/c$ further reduces e^+e^- annihilation with a hard photon from the initial state.
- ii) Between 4 and 10 outgoing charged tracks, inclusive; the upper cut again is to reduce e^+e^- annihilations.
- iii) $|z_{\text{av}}| < 8 \text{ cm}$, where z_{av} is the average z coordinate along the beam axis of all the tracks in the event, mea-

sured at their closest approach in the $R-\phi$ plane to the beam-beam interaction point; this and the next cut reduce the contamination from beam-gas interactions.

iv) The net charge of the observed tracks to be less than 4.

v) In order to facilitate the comparison with Monte Carlo simulations (Sect. 3.1), only beam energies $E_b > 16$ GeV were considered for reaction (1).

For reaction (2) we also required the following cuts:
vi) The number of charged tracks in the event to be not more than 8, and their net charge zero.

vii) The vector sum of the transverse momenta of the observed final state particles, $|\Sigma \mathbf{P}_i|$, to be less than 0.5 GeV/c.

viii) For decay mode (6), a positive and negative track, when considered as pions, to give an effective mass within 25 MeV of the K^0 , and a flight path of the K^0 in the plane perpendicular to the beam axis of at least 4 mm.

Identification of charged particles can be partly achieved by using TOF measurements. The TASSO TOF system is described elsewhere [10]. For each track which has TOF information, the square of the mass (M_{TOF}^2) is computed from the measured track length, momentum and TOF values. For each particle type i ($i = \pi, K, p$) the probabilities $W_i = C \cdot \exp(-(\tau_m - \tau_i)^2 / 2\sigma^2)$ are calculated, where τ_m is the measured TOF, τ_i the expected TOF for hypothesis i , and σ is the resolution for the time measurement. C is a normalization factor such that $\Sigma W_i = 1$. A track is defined as an identified π if $W_\pi > 0.5$, and $0.2 < P_\pi < 1.0$ GeV/c; as an identified K if $W_K > 0.9$, $0.3 < P_K < 1.0$ GeV/c and $0.1 < M_{\text{TOF}}^2 < 0.6$ GeV²; and as an identified proton if $W_p > 0.9$, $0.4 < P_p < 1.4$ GeV/c and $M_{\text{TOF}}^2 > 0.6$ GeV². A track is defined as consistent with being a $\pi(K; p)$ if it is *not* an identified K or p (π or $p; \pi$ or K).

In the following analysis, π or K consistency was required for all tracks relevant for the assumed reaction and decay. In addition we have also defined an enhanced sample of oppositely charged kaons by requiring that $W_{K^+} \cdot W_{K^-} > 0.3$ for final states involving a K^+ and a K^- .

3 Results

3.1 Inclusive $D^{*\pm}$ production

In Fig. 2, we show plots of $\Delta M = M(D^{*\pm}) - M(D^0)$ distributions, where $M(D^0)$ is the observed mass of the assumed decay products of the D^0 (selected between 1.73 and 2.00 GeV), and $M(D^{*\pm})$ is the observed mass of the D^0 and the pion in reaction (1). The data from the two decay modes (3) and (4) are presented separately. The presence of the D^* is demonstrated by the enhancement at the expected ΔM position (145.5 MeV). Fitting the data to a sum of a gaussian shape (of full width fixed at 3.0 MeV, our calculated resolution) plus a second order polynomial background yielded 13 ± 5 and 20 ± 6 events in the peak corresponding to D^* production for

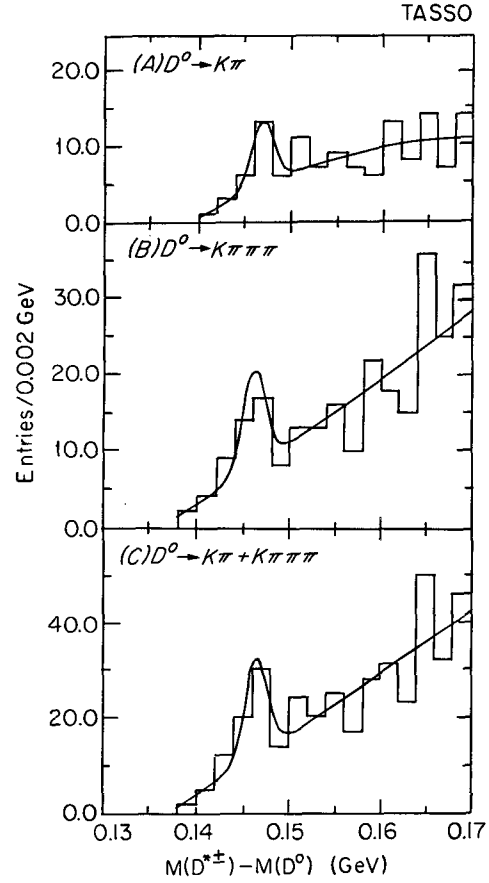


Fig. 2a-c. Plots of $\Delta M = M(D^{*\pm}) - M(D^0)$ distributions, for the inclusive data: a $D^0 \rightarrow K\pi$. b $D^0 \rightarrow K\pi\pi\pi$. c The sum of a and b. Curves are the result of fits to a second order polynomial background plus a gaussian, with a width as obtained from our calculated mass resolution

the two channels (3) and (4) respectively. The resulting ΔM values obtained in these fits are in agreement with the expected value. The use of the above form for the background is corroborated by looking at plots similar to Fig. 2a-b, with the D^0 region replaced by appropriate D^0 control regions (not shown). The shapes of the D^0 signal and control regions are similar for ΔM above 0.15 GeV, while no peak is seen below 0.15 GeV for the control regions. The statistical significance of the D^* signal is about 3 standard deviations (s.d.) in each of the above two channels. In Fig. 2c we show the combined 2a and 2b data. Here, the D^* significance is 4.0 s.d. (32 ± 8 events). All the above significances are also obtained from the difference in χ^2 between fits with and without a D^* signal.

The observed sample of D^* contains some contribution from the e^+e^- annihilation channel. Its magnitude was estimated using the standard TASSO multi-hadronic Monte Carlo, in which the generated events, normalized to the D^* signal [11] in the annihilation channel, were subjected to the same cuts as were used for selecting the D^* s from the $\gamma\gamma$ channel. In this way, the observed signal of the D^* channels was estimated to contain annihilation backgrounds originating from $e^+e^- \rightarrow c\bar{c}$ and $e^+e^- \rightarrow b\bar{b}$ of about 2 and 3 events, respectively, for the

D^0 decay modes (3) and (4). By relaxing the upper value of the $|\Sigma\mathbf{P}|$ cut (Sect. 2; cut *i*) from 10 to 13 GeV/c, the amount of annihilation background events did not change significantly.

In order to compute the inclusive cross section for the process $e^+e^- \rightarrow e^+e^- + D^{*\pm} + X$, we have used an event generator [12] which simulates the simplest production of a pair of charmed quarks by a quark-parton model (QPM) $c\bar{c}$ box diagram (Fig. 1 b), and the subsequent fragmentation into charmed hadrons according to the LUND 6.3 parton-shower model [13]. Several alternative hadronisation schemes were also used, but no significant change in the result quoted below was observed. The contribution of higher order QED radiative corrections was also calculated, and found to be negligible. All generated events were passed through a detector simulation program, and were subjected to the same cuts as imposed on the data.

Converting the background-subtracted numbers to cross sections via the calculated efficiencies, we obtain

$$\sigma(e^+e^- \rightarrow e^+e^- + D^{*\pm} + X) = 97 \pm 29 \text{ pb.}$$

For comparison, the cross section using the box diagram for a charmed quark mass of 1.6 ± 0.1 GeV, and for a $\gamma\gamma$ effective mass, $W_{\gamma\gamma}$, greater than 4.2 GeV, is calculated to be 40 ± 3 pb. Lower $W_{\gamma\gamma}$ regions down to threshold are difficult to calculate; they are estimated to contribute another 15% to the cross section. The calculation also involves the assumption that the production ratio of vector to pseudoscalar charmed mesons is [14] 3:1, and that 81% of these will be $c\bar{u}$ or $c\bar{d}$, rather than $c\bar{s}$. Thus, we see a 2 s.d. excess of events as compared with a simple quark-parton model calculation, in agreement with the JADE result [2]. Such an excess has not been seen in a preliminary result of the TPC/Two-Gamma Collaboration [3].

3.2 $D^0\bar{D}^0$ production

We have used 4 to 8 prong events to look for reaction (2), followed by decays of both neutral D mesons via modes (3)–(6). The main visible contribution to exclusive $D^0\bar{D}^0$ production in the 4 prong events is expected to come from events where the D^0 decays into $K^-\pi^+$, and the \bar{D}^0 decays either into $K^+\pi^-$, yielding two $K^\pm\pi^\mp$ combinations within a D^0 mass cut, to be defined later, per $D\bar{D}$ event, or into $K^+\pi^-\pi^0$, yielding one such combination. Our π^0 detection efficiency is too small to see a direct signal from decay mode (5) with all 3 particles detected. However, the latter decay mode is known [6] to proceed mainly via the channels $K^{*-}\pi^+$ or $K^-\rho^+$. Due to the specific angular distribution of these two channels, with the π^0 from the decay of the vector meson escaping detection, one expects to get a peak at $M(K^-\pi^+) \sim 1.55$ GeV, the so-called “satellite” peaks S^0 .

In Fig. 3a we show the distribution of $M(K^-\pi^+)$ for the 4-prong events, when the *other* $M(K\pi)$ combination is either in the D^0 mass region (1.73–2.00 GeV), with the event $|\Sigma\mathbf{P}_T|$ smaller than 0.2 GeV/c, or when it is

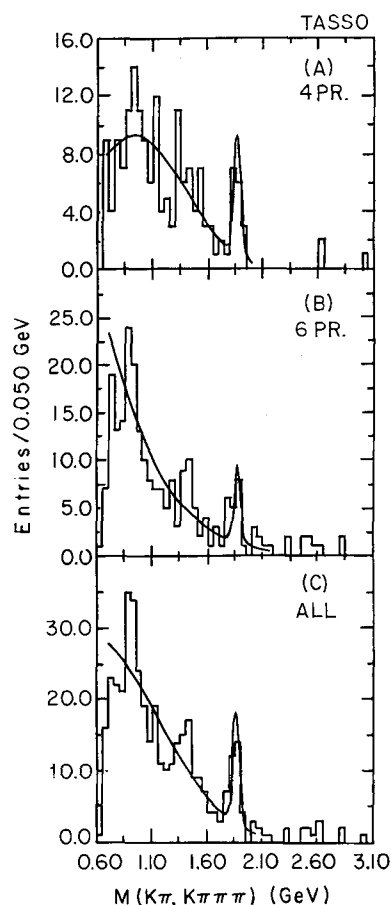


Fig. 3. **a** $M(K\pi)$ distribution recoiling against $M(K\pi)$ in the D^0 region, for $|\Sigma\mathbf{P}_T| \leq 0.2$ GeV/c; or $M(K\pi)$ in the S^0 region, for $|\Sigma\mathbf{P}_T| = 0.1-0.5$ GeV/c, 4 prong data. **b** $M(K\pi)$ or $M(K3\pi)$ recoiling against $M(K3\pi)$ or $M(K\pi)$ respectively in the D^0 region, for $|\Sigma\mathbf{P}_T| \leq 0.35$ GeV/c, 6 prong data. See text for exact cuts. **c** Sum of **a** and **b**. Curves are fits to the data using a sum of an exponential ($\exp[AM + BM^2]$) background shape and a gaussian resonance at the D^0 mass (1.865 GeV) and width determined from our calculated mass resolution (0.07 GeV full width at half-maximum)

in the S^0 region (1.45–1.65 GeV), with $|\Sigma\mathbf{P}_T|$ between 0.1 and 0.5 GeV/c. Monte Carlo studies indicate that the cleanest S^0 peak for $D\bar{D}$ production at our energies is obtained when one selects the $|\Sigma\mathbf{P}_T|$ of the event to be in the above range. A clear D^0 peak is seen, with almost no background (Fig. 3a).

We have looked for a $D^0\bar{D}^0$ signal in the 6-prong events, when one D^0 decays via mode (3) and the other via mode (4). In Fig. 3b we show the $M(K\pi)(M(K3\pi))$ distribution when the complementary $M(K3\pi)(M(K\pi))$ combination is in the D^0 region, for $|\Sigma\mathbf{P}_T| < 0.35$ GeV/c. Our Monte Carlo shows that this $|\Sigma\mathbf{P}_T|$ cut is more suitable for the 6-prong events. A D^0 peak is seen, over a small background. Due to the larger combinatorial background (in accordance with Monte Carlo expectations), no satellite peak could be obtained for these data.

The data of Fig. 3 were fitted to a sum of an exponential background shape of the form ($\exp[AM + BM^2]$) and a gaussian D^0 of a mass 1.865 GeV and a full width 0.07 GeV, determined from our calculated mass resolu-

tion. The fit yielded $12.4 \pm 3.6 D^0 \bar{D}^0$ entries in the 4 prong data, and 12.1 ± 3.8 events in the 6 prongs (statistical errors only). For the $D^0 \bar{D}^0$ events, the contribution from $e^+ e^-$ annihilations is negligible. Also here, a D^0 control region ($M = 2.00 - 2.27$ GeV) gave no D^0 recoil peak. The combined fit (Fig. 3c) yields a significance of over 4 s.d. (23 ± 5 events). The same significance is obtained from the difference in the χ^2 of the fits with and without a D^0 signal. Both the 4- and 6-prong signals populate $W_{\gamma\gamma}$ regions within 1 GeV above the kinematical threshold. The low mass peaks in Fig. 3c are consistent with $K^*(892)$ and $K_2^*(1430)$ production in this data sample. Including these two resonances in the fit of Fig. 3c does not alter the number of D^0 events, but improves the goodness of fit.

Events where both neutral D mesons decay via the mode (4) result in 8 prong events. In this case the large number of combinatorial possibilities makes the background too large. We have also searched for a combination of modes (3) and (6) among the 6 prong events and (3) and (5) in the 4 prong data. The need to observe the $\bar{K}^0 \rightarrow \pi^+ \pi^-$ decay in reaction (6) and the π^0 in reaction (5) results in a low efficiency and a small expected number of events; our data are consistent with this.

In order to determine the cross section for the above $D^0 \bar{D}^0$ signal, Monte Carlo simulations have been used, incorporating the full kinematics of the $\gamma\gamma$ system, generated according to the flux of transverse photons, using the formulae of [15]. As for reaction (1), all generated events were passed through a detector simulation program, and were subjected to the same cuts as imposed on the data.

Despite seeing a clear $D^0 \bar{D}^0$ signal, we cannot conclude that this is due to exclusive $D^0 \bar{D}^0$ production. An extra source of such events is $D^{*0} \bar{D}^0$ or $D^{*0} \bar{D}^{*0}$ production, with $D^{*0} \rightarrow D^0 \pi^0$ or $D^0 \gamma$. Because the γ and π^0 are of very low momentum, many of these events pass our $|\Sigma P_{\perp i}|$ cuts, and hence appear as $D^0 \bar{D}^0$ events. Monte Carlo studies show that with our cuts the efficiency for accepting $D^0 \bar{D}^0$, $D^0 \bar{D}^{*0}$ and $D^{*0} \bar{D}^{*0}$ events differ only by a factor of 0.8. Thus we are unable to determine what fraction of our observed events are due to $D^0 \bar{D}^0$, $D^{*0} \bar{D}^0$ and $D^{*0} \bar{D}^{*0}$.

The main contribution to reaction (2) stems from the reactions $\gamma\gamma \rightarrow D^0 \bar{D}^0$, $D^0 \bar{D}^{*0}$, and $D^{*0} \bar{D}^{*0}$. Assuming the ratio of vector to pseudoscalar production to be [14] $D^{*0}:D^0 = 3:1$, the production ratios of the reactions

$$\begin{aligned} \gamma + \gamma &\rightarrow D^{*0} + \bar{D}^{*0} \\ \gamma + \gamma &\rightarrow D^{*0} + \bar{D}^0 \quad \text{or} \quad \bar{D}^{*0} + D^0 \\ \gamma + \gamma &\rightarrow D^0 + \bar{D}^0 \end{aligned}$$

are expected to be 9:6:1. $D^{*\pm}$ and D^\pm are also expected to be produced with the same relative ratios. However, an overall reduction factor of $D^{*\pm}$ and D^\pm compared to D^{*0} and D^0 may occur, depending on the exact D , D^* production mechanism. Since the photon coupling to quarks is proportional to e_q^2 , the D charge to neutral ratio can vary between 1:1 in diagrams where the photons are coupled only to c -quarks (Fig. 1b) and 1:16

in diagrams where the photons are coupled to u or d quarks (Fig. 1c). Brodsky et al. [16] estimate this ratio to be $\approx 1:8$. Monte Carlo simulations show that for our experimental conditions (4 and 6 prong events at the above $|\Sigma P_{\perp i}|$ regions), the efficiency for accepting D^0 mesons originating from charged compared to neutral D^* and D mesons is very small, and thus the charged D^* contribution to $D^0 \bar{D}^0$ production was neglected.

The experimental cross section for reaction (2) for visible $W_{\gamma\gamma}$ values within 1 GeV above threshold was obtained by using Monte Carlo simulations of the above 3 channels, weighted according to the production ratios assumed above. The result is

$$\sigma(\gamma\gamma \rightarrow D^0 \bar{D}^0 (+X)) = 56 \pm 13(\text{stat.}) \pm 12(\text{syst.}) \text{ nb.}$$

The systematic error includes uncertainties in the contributions of the relative cross sections of the various reactions, the fits and Monte Carlo calculations. Due to the similar acceptances of the 3 channels, this result is not too sensitive to the D^*/D production ratio. Note also that the result will not change much if other channels are contributing to reaction (2) within the above cuts with similar detection efficiencies.

4 Summary and discussion

We have seen evidence for inclusive $D^{*\pm}$ production in $\gamma\gamma$ collisions with a significance of about 3 standard deviations in each of the two decay channels (3) and (4). We measure the following cross section: $\sigma(e^+ e^- \rightarrow e^+ e^- + D^{*\pm} + X) = 97 \pm 29$ pb. This can be compared with a simple QPM expectation of about 46 pb. Such an excess is consistent with an earlier observation [2], and may also be related to the excess of events seen [17] in single inclusive particle production at high P_T in photon-photon collisions.

We have observed a signal in the region expected for $D^0 \bar{D}^0$ exclusive production, but are unable to exclude the possibility that in part this originates from D^{*0} decays. Our measurement of the cross section for the reaction $\gamma\gamma \rightarrow D^0 \bar{D}^0 (+X)$ is $56 \pm 13 \pm 12$ nb. This cross section is much larger than predicted by a simple model [16] which computes strictly exclusive two-body channels. Note that this model underestimates the $K^{*+} K^{*-}$ cross section of [5].

The total charm production cross section in photon-photon collisions can be estimated as follows:

a) Prompt *neutral* meson pair production is given by the above cross section for reaction (2), after subtracting the small contribution to this reaction due to prompt $D^{*+} D^{*-}$ production. For equal production of charged and neutral $D^*(D)$ mesons as in Fig. 1b, this contribution is estimated from Monte Carlo studies to be $\approx 6\%$, yielding for prompt neutral meson pair production $\sigma = 53 \pm 13$ nb (statistical error only).

b) We assume that not far from threshold, prompt *charged* meson pair production comes mainly from the exclusive reactions $\gamma\gamma \rightarrow D^{*+} D^{*-}$, $D^{*+} D^-$ and $D^+ D^-$ in the ratio of 9:6:1. Having extra pions will not change

the result substantially. With the above assumption, comparing Monte Carlo generated events of these exclusive channels with the inclusive $D^{*\pm}$ measurement of Sect. 3.1, we obtain a cross section for prompt charged meson pair production $\sigma = 61 \pm 17$ nb (statistical error only).

These results indicate similar cross sections for prompt charged and neutral meson pair production at visible $W_{\gamma\gamma}$ values within 1 GeV above threshold. This is consistent with the prediction of Fig. 1 b. Assuming as in Sect. 3.1 that only $\approx 81\%$ of charm production is accounted for by D and D^* mesons, we estimate the total charm cross section near threshold to be $\sigma(\gamma\gamma \rightarrow \text{charm}) \approx 141$ nb. This cross section may even be larger if reactions like $\gamma\gamma \rightarrow D^{*+} \bar{D}^{*0} \pi^-$ contribute significantly to charm production near threshold. Thus, with all the above assumptions, the overall charm production seems to constitute a sizable fraction of the total $\gamma\gamma$ hadronic cross section [18], which is ≈ 400 nb in the above $W_{\gamma\gamma}$ range. This is consistent with the assumption that a major part of $\sigma^{\text{tot}}(\gamma\gamma \rightarrow \text{hadrons})$ is governed by the two-photon coupling to quarks, which is proportional to the fourth power of the quark charge. The large charm cross section, probably dominated by $D^* \bar{D}^*$ production, is reminiscent of the high rates near threshold found for other $\gamma\gamma \rightarrow$ two vector meson states [4, 5].

Acknowledgement. We gratefully acknowledge the support of the DESY Directorate, the PETRA machine group and the DESY computer centre. Those of us from outside DESY wish to thank the DESY Directorate for the hospitality extended to us while working at DESY. We also thank Mrs. T. Gilead, Mrs. H. Katz, and Mrs. B. Peled for their invaluable help in processing the two-photon data and Monte Carlo samples.

References

1. PLUTO Coll. Ch. Berger et al.: Phys. Lett. 167B (1986) 120; R 704 Coll. C. Baglin et al.: Phys. Lett. 187B (1987) 191; TPC/Two-Gamma Coll. H. Aihara et al.: Phys. Rev. Lett. 60 (1988) 2355; TASSO Coll., W. Braunschweig et al.: Z. Phys. C – Particles and Fields 41 (1989) 533
2. W. Bartel et al.: Phys. Lett. B184 (1987) 288; A.J. Finch, in: Proceedings of the VIII International Workshop on Photon-Photon Collisions, Shresh, Israel (1988), U. Karshon (ed) p. 75. Singapore: World Scientific 1988
3. H. Aihara et al.: Submitted to 1987 Int. Symp. on Lepton and Photon Interactions at High Energies, Hamburg 1987; F.C. Erne, in: Proceedings of the VIII International Workshop on Photon-Photon Collisions, *ibid.*, p. 71 (1988)
4. TASSO Coll. R. Brandelik et al.: Phys. Lett. 97B (1980) 448; MARKII Coll. D.L. Burke et al.: Phys. Lett. 103 B (1981) 153; TASSO Coll. M. Althoff et al.: Z. Phys. C – Particles and Fields 16 (1982) 13; CELLO Coll. H.J. Behrend et al.: Z. Phys. C – Particles and Fields 21 (1984) 205; TPC/Two-Gamma Coll. H. Aihara et al.: Phys. Rev. D37 (1988) 28; PLUTO Coll. Ch. Berger et al.: Z. Phys. C – Particles and Fields 38 (1988) 521; For a recent review of $\rho^0 \rho^0$ cross sections see A.W. Nilsson in Proceedings of the VIII International Workshop on Photon-Photon Collisions, *ibid.*, p. 261 (1988)
5. ARGUS Coll. H. Albrecht et al.: Phys. Lett. B212 (1988) 528
6. Particle Data Group: Phys. Lett. B204 (1988) 1
7. TASSO Coll. R. Brandelik et al.: Phys. Lett. 83B (1979) 261; Z. Phys. C – Particles and Fields 4 (1980) 87
8. TASSO Coll. M. Althoff et al.: Phys. Lett. 141 B (1984) 264
9. TASSO Coll. M. Althoff et al.: Phys. Lett. 126B (1983) 493
10. TASSO Coll. M. Althoff et al.: Z. Phys. C – Particles and Fields 32 (1986) 11
11. TASSO Coll. W. Braunschweig et al.: Z. Phys. C – Particles and Fields 44 (1989) 365
12. F.H. Berends, P.H. Daverveldt, R. Kleis: Comput. Phys. Commun. 40 (1986) 271; 40 (1986) 285; 40 (1986) 309
13. T. Sjöstrand: Comput. Phys. Commun. 39 (1986) 347; T. Sjöstrand, M. Bengtsson: Comput. Phys. Commun. 43 (1987) 367
14. J. Adler et al. MK III Coll.: Phys. Lett. B208 (1988) 152; de Rujula et al.: Phys. Rev. Lett. 37 (1976) 398
15. V.M. Budnev et al.: Phys. Rep. 15 (1975) 181
16. S.J. Brodsky, G. Köpp, P.M. Zerwas: Phys. Rev. Lett. 58 (1987) 443
17. TASSO Coll. R. Brandelik et al.: Phys. Lett. 107B (1981) 290; TASSO Coll. M. Althoff et al.: Phys. Lett. 138B (1984) 219; PLUTO Coll. Ch. Berger et al.: Z. Phys. C – Particles and Fields 26 (1984) 191; 29 (1985) 499
18. PLUTO Coll. Ch. Berger et al.: Z. Phys. C – Particles and Fields 26 (1984) 353; D. Bintinger et al.: Phys. Rev. Lett. 54 (1985) 763; S.E. Baru et al.: Novosibirsk preprint 86–106 (1986); M. Feindt, in: Proceedings of the VII International Workshop on Photon-Photon Collisions, Paris (1986), A. Courau, P. Kessler (eds) p. 388. Singapore: World Scientific 1986; TPC/Two-Gamma Coll. H. Aihara et al.: SLAC-PUB-5101, 1989; For a recent compilation of $\sigma_{\text{tot}}(\gamma\gamma \rightarrow \text{hadrons})$ see J.H. Field in Proceedings of the VIII International Workshop on Photon-Photon Collisions, *ibid.*, p. 360 (1988)